Adsorption and Decomposition of NO on Magnesium Oxide: A Quantum Chemical Study

Xin Lu, Xin Xu,* Nanqin Wang, and Qianer Zhang

State Key Laboratory for Physical Chemistry of Solid Surfaces; Institute of Physical Chemistry, Department of Chemistry, Xiamen University, Xiamen 361005, PR China

Received: November 10, 1998

Embedded cluster model calculations based on density functional theory have been used to study the adsorption of NO on MgO surface. The calculation results indicate that at ideal terrace sites on MgO(100) surface, NO is weakly adsorbed as NO and *cis*-N_2O_2, whereas at step and corner sites NO could be adsorbed as (a) NO adspecies with N-end bridging over the step-sitting Mg_{XC}-O_{YC} (X,Y = 3,4) ion pairs, (b) NO_2^{2-} adspecies with the O−N bond of the adsorbed NO molecule chaining over the step-sitting Mg_{XC}-O_{YC} (X,Y = 3,4) ion pairs, and (c) $N_2O_3^{2-}$ adspecies by attaching another NO molecule onto the NO_2^{2-} adspecies. The latter species could be regarded as an intermediate for NO decomposition over MgO catalyst. The calculated IR frequencies of the weakly adsorbed *cis*-N_2O_2 species and the chemisorption-induced NO_2^{2-} and $N_2O_3^{2-}$ surface species agree well with those from the IR experiments. On the basis of the calculated energetics, a possible mechanism of NO decomposition reaction has been proposed.

1. Introduction

The mechanistic understanding of catalytic decomposition and reduction of NO_x is of great importance in pollution control. Accordingly, there exist numerous experimental investigations on the interactions of nitric oxide with metals and metal oxides. For NO decomposition on metallic catalysts, two mechanisms have been proposed,[1−4] via dissociative adsorption of NO and via the activation of the adsorbed $(NO)_2$ dimers to form N_2O. For NO decomposition on metal oxide surfaces, the mechanism is not well-known, despite the fact that there have been several experimental efforts on this topic, from the earlier systematic work of Winter[5,6] to the very recent work of Acke et al.[7]

Practically, NO is known as a probe molecule, whereas MgO is generally believed to have the most stable, well-defined (100) surfaces exposed, and is always used as the prototype of metal oxide catalysts. It was found that the chemisorption of NO on MgO powders leads to the decomposition of NO to N_2 and O_2, and the formation of N_2O.[5,6,8−11] The coordinatively unsaturated anions at steps and kinks were suggested to play an important role in NO chemisorption and in the relevant catalytic process. Gravimetric determinations indicated that the NO coverage on MgO (per $Mg^{2+}O^{2-}$ ion pair) at room temperature (RT) is roughly 0.04−0.05, implying that NO chemisorption should occur at the corner and step sites.[9] On the basis of the IR[8,9] and ESR[12,13] spectra, a variety of surface complexes such as NO^-, NO_2^{2-}, *cis*-$N_2O_2^{2-}$, and *cis*-N_2O_2 have been proposed to exist on the surfaces of NO-preadsorbed MgO catalyst. Among them, the *cis*-$N_2O_2^{2-}$, as well as NO_2^-, was postulated to be formed via a disproportionation reaction and to work as a pivot intermediate in the thermal decomposition of NO on MgO.[8,9] This hypothesis had been utilized to account for the complex absorptions in the range of 1500−1350 cm^{-1} and 1250−1100 cm^{-1} in the IR spectra of NO/MgO adsorption system.[8,9] However, these specific IR bands appeared even at rather low temperature (77 K).[9] It seems unlikely that the slow disproportionation reaction could give rise to the so-called "$N_2O_2^{2-}$" and "NO_2^-" species at such low temperature of 77 K.[14] This brings up the questions of whether the so-called "$N_2O_2^{2-}$" does exist in the NO/MgO chemisorption system as an intermediate of the NO decomposition reaction, and in what form(s) the real intermediate(s) could be. In this respect, a systematic quantum chemical study of the NO/MgO chemisorption system should be of particular help for the mechanistic understanding of the specific process.

No detailed theoretical work has been done on the NO/MgO system. While we were preparing this manuscript, Snis and Panas reported a related work on NO/CaO.[16] By means of the regularized complete active space self-consistent field method (reg-CASSCF) and the complete active space second-order perturbation theory (CASPT2), they have investigated the relative adsorption reactivities over various surface sites of CaO. The adsorption of anionic NO and N_2O_2 onto Ca and O surface atoms, an oxygen vacancy, and to two different edge sites have been examined and implications of excess surface electrons to heterogeneous NO reduction processes have also been discussed.[16] The calculated frequencies of the anionic surface species were compared with the available experimental IR spectra.[16]

In a previous paper, we reported a preliminary first principle study regarding monomeric NO adsorption at 5,4,3-coordinate surface sites on MgO solid by using bare $(MgO)_n$ (n = 4, 6, 9) cluster models.[15] In the present paper, a systematic first principle embedded cluster modeling of the NO/MgO chemisorption system are reported. We aim to address the following questions: (a) How does NO adsorb on MgO surfaces? (b) What kinds of surface species work as intermediates in NO decomposition and by which way are the intermediates produced? To answer these questions, we have considered the adsorptions of some possible species, including NO and $(NO)_2$, at the terrace, step, corner, and island sites of MgO(100) surface. IR frequencies of the surface species considered have been calculated and compared with the experimental IR spectra. On the basis of the calculated energetics, a possible mechanism of NO decomposition reaction has been proposed.

* Corresponding author. E-mail address: xinxu@xmu.edu.cn.

10.1021/jp984387s CCC: $18.00
Published on Web 06/19/1999

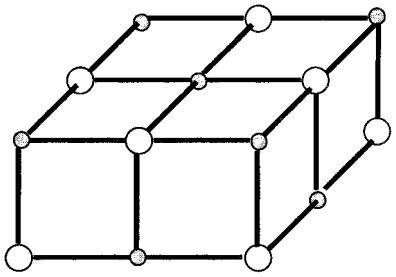

Figure 1. $(MgO)_9$ (C_{4V}) cluster to model Mg_{5C} (or O_{5C}) site on MgO-(100). The surrounding 708 ($11 \times 11 \times 6 - 18$) point charges ($\pm 1.75$) as well as the Ne-core potentials on the bordering positive point charges are not shown here. (To model Mg_{5C} site, the black dot is Mg, and the white circle is O. To model O_{5C} site, the black dot is O atom, and the white circle is Mg.)

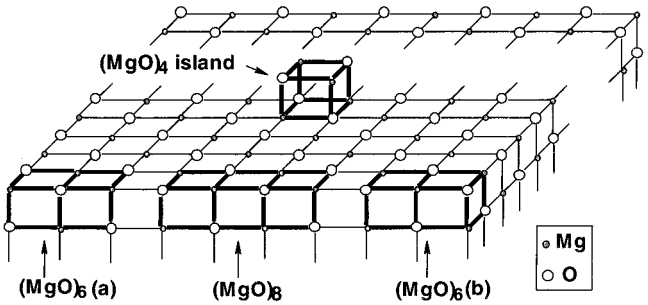

Figure 2. The low-coordinate sites on a ($10 \times 10 \times 10$) microcrystal as well as the corresponding embedded cluster models.

2. Computational Details

Solid MgO has a rock salt structure with the most stable, well-defined (100) surface exposed.[17] For the five-coordinate Mg cation site or O anion site on MgO(100) surface, a $(MgO)_9$ cluster in the C_{4V} point group symmetry (Figure 1) was used with the superficial, central atom being Mg or O, respectively. These clusters are then embedded within an array of 708 ($11 \times 11 \times 6 - 18 = 708$) point charges (PCs). Lower-coordinate sites were simulated by a series of $(MgO)_n$ ($n = 4, 6, 8$), which were placed on the surface or at the corner and edge of a ($10 \times 10 \times 10$) microcrystal respectively, as depicted in Figure 2. As such, we have four embedded cluster models. They are $(MgO)_4$ island at the center of the (100) surface with both O_{3C} and Mg_{3C} exposed, $(MgO)_6$(a) at corner site with an O_{3C} anion and a Mg_{4C} cation exposed, $(MgO)_6$(b) at corner site with an O_{4C} anion and a Mg_{3C} cation exposed, and $(MgO)_8$ at step site with an O_{4C} anion and a Mg_{4C} cation exposed.

To circumvent artificial polarization on the in-cluster anions induced by the bordering positive PCs, the boundary positive charges were further augmented with Ne-core effective potentials of Mg.[18] The values of PCs are ± 1.75, which were determined self-consistently in a previous study.[19] In all calculations throughout, the nearest Mg−O distance within these surface clusters was fixed at its bulk value of 2.104 Å.[17] Some other cluster models have also been used and will be specified in the text.

Calculations were performed with the hybrid B3LYP density functional method[20,21] implemented in the *Gaussian 94* suite of program.[22] B3LYP refers to Becke's three-parameter hybrid method,[20] using the correlation functional from Lee, et al.[21] For O and N, we used the standard 6-31+G* basis sets.[22] For Mg, we used the 6-31G* basis set.[22] For free NO molecule, the N−O bond length and the dissociation energy calculated with B3LYP method are 1.158 Å and 150.7 kcal/mol, in good agreement with the experimental values of 1.151 Å and 150.1 kcal/mol, respectively.[23] We have applied the counterpoise method to account for the basis set superposition errors (BSSE) for the calculations of binding energies.[24]

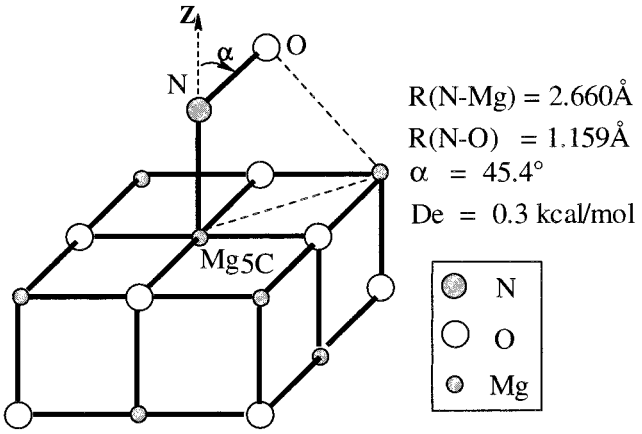

Figure 3. NO adsorption on the Mg_{5C} site modeled by an embedded $(MgO)_9$ cluster.

IR frequencies reported here were calculated by using bare cluster models to simulate the specific adsorptive surface sites. The calculated frequencies seem to be in good agreement with the experimental IR spectra. Interestingly, we also noticed that in a previous paper by Coluccia and colleagues, reasonable prediction of the frequency shifts for CO adsorptions on the three-, four-, and five-coordinate cations on MgO (100) surfaces was reached by using $(MgO)_n$ ($n = 4, 6, 9, 12$) bare cluster models.[25]

3. Results and Discussion

3.1. NO Adsorption on Terrace Site. For single NO molecule adsorption on terrace sites, four adsorption modes, that is, NO with N-end or O-end down on Mg_{5C} site, and with N-end or O-end down on O_{5C}, have been considered. Only the first adsorption mode is found to result in a weak, attractive interaction between the adsorbed NO and the substrate. For the other three modes, the interactions between NO and the surface are all virtually repulsive. The optimized geometry of NO adsorption with N-end down on the Mg_{5C} terrace site is depicted in Figure 3, which clearly shows that the adsorbed NO molecule tilts away from the surface normal by an angle of 45.4°. Free NO molecule is known to have a $^2\Pi$ ground state, whereas the $(MgO)_9$ embedded cluster has a close-shell configuration. With the tilted adsorption geometry, the adsorption system, that is, NO + $(MgO)_9$ embedded cluster, has a $^2A''$ ground state. The long N−Mg_{5C} distance (2.660 Å), the undistorted intramolecular N−O bond length (1.158 Å), and the low binding energy (0.3 kcal/mol and 0.1 kcal/mol before and after BSSE correction, respectively) infer that NO is reversibly physisorbed, and must be highly mobile on the surface even at rather low temperature. As each NO admolecule has an unpaired electron, this high mobility on the surface may facilitate NO dimerization, giving rise to the formation of N_2O_2 adspecies.

3.2. *cis*-N_2O_2 Adsorption on Mg_{5C}-Mg_{5C} Pair Site. Platero et al. have detected abundant *cis*-N_2O_2 dimers on MgO at 77 K by means of IR spectroscopy. On the basis of some structural arguments, they supposed that the cis dimer should adsorb on the Mg_{5C}-Mg_{5C} pair site of MgO(100) in the distance of 4.21 Å.[9] This, however, seems unlikely, because there is an O^{2-} anion between the two cations of such pair site, and the incoming *cis*-N_2O_2 should thus experience a strong repulsion from the central O^{2-} anion. We have modeled the Mg_{5C}-O_{5C}-Mg_{5C}

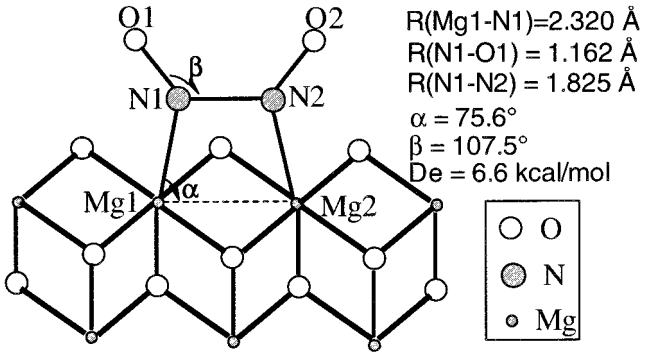

Figure 4. Optimized geometry of *cis*-N_2O_2 adsorbed on a Mg_{5C}-Mg_{5C} pair. [The surrounding of the $(MgO)_{10}$ cluster is not shown.]

surface site with embedded $(MgO)_9$ cluster. No stable *cis*-N_2O_2 adspecies could be found.

It seems more reasonable to assume that the *cis*-N_2O_2 would be adsorbed on a pair site of Mg_{5C}-Mg_{5C} in the distance of 2.975 Å (see Figure 4). The Mg and O atoms in the central part of the $(MgO)_{10}$ cluster model, that is, the central cubic $(MgO)_4$, were described with 6-31G* and 6-31+G*,[22] respectively, whereas the rest in-cluster Mg and O atoms were described with CEP-31G[18] with Ne-core potential and He-core potential, respectively. The N and O atoms in NO were described with 6-31+G*. [22]

Free NO dimer has been extensively studied,[26−36] and has been shown to be a challenge to theoreticians and experimentalists. Most of the theoretical (HF, post-HF, and DFT) methods meet with difficulty in reproducing the geometry, binding energy, ground-state electronic configuration, and vibrational frequencies of the NO dimer.[26−35] Our B3LYP calculations revealed that free *cis*-N_2O_2 molecule has two low-lying states, that is, triplet and singlet states, among which the singlet state $^1A_1$ is by 2 kcal/mol less stable than the ground triplet state $^3B_1$, and the NO−NO binding energy in the *cis*-N_2O_2 ($^3B_1$) is only ∼ 0.03 kcal/mol with respect to the NO($^2\Pi$) + NO($^2\Pi$) asymptote. These outcomes agree with the previous DFT calculations,[29−35] but somewhat contradict the existing post-HF findings.[27,28] As the substrate−adsorbate interaction would possibly change the triplet−singlet splitting of *cis*-N_2O_2, it is necessary to consider *cis*-N_2O_2 adsorption both in triplet and in singlet on the Mg_{5C}-Mg_{5C} pair site. However, no stable *cis*-N_2O_2 adspecies could be located for the triplet state.

Figure 4 presents the optimized geometry for the adsorbed *cis*-N_2O_2 in singlet state. The optimal N−N bond length is 1.825 Å, about 0.13 Å shorter than that of 1.960 Å in the singlet state ($^1A_1$) of free *cis*-N_2O_2. The intramolecular N−O bond length, 1.162 Å, is slightly elongated upon adsorption and dimerization, with respect to free NO molecule (1.158 Å). The nearest N−Mg_{5C} distance is 2.32 Å, by about 0.34 Å shorter than the N−Mg_{5C} distance of 2.66 Å for the monomeric adsorption. The calculated binding energy with respect to two free NO molecules is 6.6 kcal/mol without the BSSE correction and 1.4 kcal/mol after the BSSE correction has been taken into account. This gives an average value of 3.3 kcal/mol without the BSSE correction, or 0.7 kcal/mol with BSSE correction, per NO molecule. Therefore, NO adsorption on MgO(100) surface in the form of *cis*-N_2O_2 is more stable than the monomeric adsorption. However, the yet low average binding energy infers that *cis*-N_2O_2 is just physisorbed on the cation−cation pair site and could hardly exist at RT. This inference is in accordance with the experimental observation that at 77 K the IR peaks ascribed to physisorbed *cis*-N_2O_2 decrease and eventually

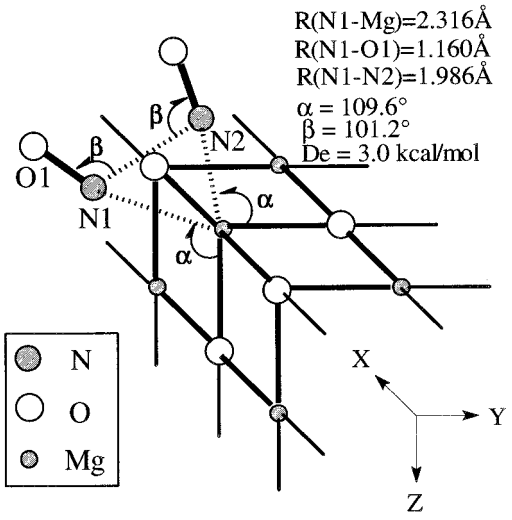

Figure 5. *Cis*-N_2O_2 adspecies on a step-sitting Mg_{4C} cation site modeled by a $(MgO)_6$ cluster embedded at the edge of a (11 × 6 × 6) microcrystal. (The whole system has the C_{2V} symmetry.)

disappear even upon outgassing.[9] Apart from the *cis*-N_2O_2 adspecies formed on the Mg_{5C}-Mg_{5C} pair site, Platero et al. also supposed that the *cis*-N_2O_2 could adsorb on a low-coordinate cation, for example, a step-sitting, four-coordinate cation (i.e., Mg_{4C}).[9] We have checked this possibility and the calculation results are given in the next subsection.

3.3. *Cis*-N_2O_2 Adsorption on Mg_{4C} Step Site. The step-sitting Mg_{4C} site was modeled by a $(MgO)_6$ cutoff cluster located at the edge of an (11 × 6 × 6) microcrystal (Figure 5). Two possible configurations of *cis*-N_2O_2 adsorbed on the Mg_{4C} site have been considered. In the first mode, the N1−N2 bond of *cis*-N_2O_2 is parallel to the O_{4C}-Mg_{4C}-O_{4C} edge whereas in the second mode, the N1−N2 bond of *cis*-N_2O_2 is perpendicular to the O_{4C}-Mg_{4C}-O_{4C} edge. The local symmetry of the cluster models is in C_{2V}. Our calculations suggest that the second mode is energetically favorable, the optimal geometry of which is shown in Figure 5. As compared with the adsorption geometry on the Mg_{5C}-Mg_{5C} pair site, the adsorption on the Mg_{4C} site leads to a shorter N−Mg distance, but a longer N−N distance, suggesting a weaker N−N bonding for *cis*-N_2O_2 adsorption on the edge site. The calculated binding energy of *cis*-N_2O_2/Mg_{4C} is about 3.0 kcal/mol with respect to two free NO molecules, which is similar to that of *cis*-N_2O_2/Mg_{5C}-Mg_{5C}. The BSSE-corrected value of this property is 1.7 kcal/mol, by 0.3 kcal/mol higher than that of *cis*-N_2O_2/Mg_{5C}-Mg_{5C}.

Experimentally, at 77 K the intensities of the IR bands owing to *cis*-N_2O_2/Mg_{4C} were found to be less sensitive to outgassing than those owing to *cis*-N_2O_2/Mg_{5C}-Mg_{5C}.[9] This observation would be rationalized by the argument that the lateral repulsion between the adspecies on the Mg_{5C}-Mg_{5C} cation pair sites should be larger than that between the adspecies on the step-sitting Mg_{4C} sites. Note that the distance between the nearest cation−cation pair sites is 2.975 Å on MgO(100), whereas at the edge, the distance between two nearest Mg_{4C} sites is 4.21 Å. Hence *cis*-N_2O_2/Mg_{5C}-Mg_{5C} could be more destabilized because of the larger lateral repulsion.

3.4. IR Frequencies of *cis*-N_2O_2 Adspecies. Experimentally, four absorption peaks in the range of 1900−1750 were detected on MgO after NO adsorption at 77 K.[9] The peaks at 1896 and 1810 cm^{-1} were ascribed to *cis*-N_2O_2 adsorbed on Mg_{4C} at the edge, and the peaks at 1866 and 1745 cm^{-1} were attributed to *cis*-N_2O_2 adsorbed on two Mg_{5C} in the distance of 4.21 Å on MgO(100). We have shown in subsection 3.2, however, that

TABLE 1: Calculated and Experimental IR Frequencies (cm^{-1}) of the *cis*-N_2O_2 Adspecies

adsorption site		ν_1 (sym.)	ν_2 (asym.)
Mg−Mg pair site	B3LYP	1877	1813
	expt. (77 K)[a]	1866	1745
Mg_{4C}	B3LYP	1918	1781
	expt. (77 K)[a]	1896	1810

[a] Experimental values extracted from ref 9.

the pair site of Mg_{5C} cations in the distance of 2.975 Å should be a better candidate for the *cis*-N_2O_2 adsorption on Mg_{5C}-Mg_{5C} pair site of MgO(100).

To calculate the IR frequencies of the adsorbed *cis*-N_2O_2, two bare cluster models, $(MgO)_{10}$ (local symmetry: C_{2V}) and $(MgO)_6$ (local symmetry: D_{2h}) are used to model these two types of surface sites, respectively. The calculated binding energies for *cis*-N_2O_2 on the two bare cluster models are 3.4 kcal/mol and 7.7 kcal/mol, respectively. These values are slightly larger than those obtained by using embedded cluster models. The calculated frequencies of the symmetric and asymmetric stretching modes of *cis*-N_2O_2 adspecies are given in Table 1, where we also include the corresponding experimental IR frequencies for comparison.[9] The calculated IR frequencies are comparable with the corresponding experimental values.

3.5. NO Monomeric Adsorption on Step, Corner, and Island. For the monomeric adsorptions of NO at the island, corner, and step sites, two adsorption modes have been found in our calculations. These are the bridge mode with NO bridging over the Mg_{XC}-O_{YC} (X,Y = 3,4) bond (see Figure 6 a−d) and the chain mode with NO lying over the O_{YC}-Mg_{XC} bond (see Figure 7 (a−d). All these systems are in the state of $^2A''$ with the spin-unpaired electron localized on the NO adspecies. In particular, the unpaired electron is localized on the N atom of the adsorbed NO in the chain mode. Table 2 summarizes the calculated geometrical parameters and binding energies for the monomeric NO adsorptions.

In the bridge mode, the calculated N−Mg_{XC} (X = 3,4) distances range from 2.102 Å (over Mg_{3C}-O_{3C}) to 2.243 Å (over Mg_{4C}-O_{4C}) whereas the N−O_{YC} distances are between 2.109 Å and 2.328 Å. The higher coordination number the active site has, the longer N−Mg_{XC} and N−O_{YC} distances are. On the basis of the calculated binding energies, which range from 17.9 kcal/mol on Mg_{3C}-O_{3C} to 7.0 kcal/mol on Mg_{4C}-O_{4C}, the strengths of NO adsorptions in the bridge mode over the Mg_{XC}-O_{YC} pair sites could be assigned as following the order of Mg_{3C}-O_{3C} > Mg_{3C}-O_{4C} > Mg_{4C}-O_{3C} > Mg_{4C}-O_{4C}. BSSE effect is trivial for these monomeric adsorptions, and thus BSSE correction does not alter the order of reactivity drawn above without BSSE correction (c.f. Table 2).

Detailed Mulliken population and Natural Bond Orbital (NBO) analyses[37] indicate that for NO adsorbed in the bridge mode, there exists a weak electron transfer from NO 5σ to the empty atomic orbitals of Mg_{XC} cation, and concomitantly a weak electron back-donation from the lone pair on O_{YC} to the empty 2π* of NO. NO is found to be only slightly negatively charged upon adsorption in the bridge mode (cf. Table 2). This result, combined with the feature that the intramolecular N−O bond is only slightly elongated by 0.01−0.02 Å upon adsorption, informs us that NO adsorbed in the bridge mode is not highly activated.

When NO is adsorbed in the chain mode, things become much different. The distances between the N atoms of NO adspecies and the O_{YC} active sites are much shorter, within the range of 1.53−1.63 Å. This indicates the formation of a covalent bond

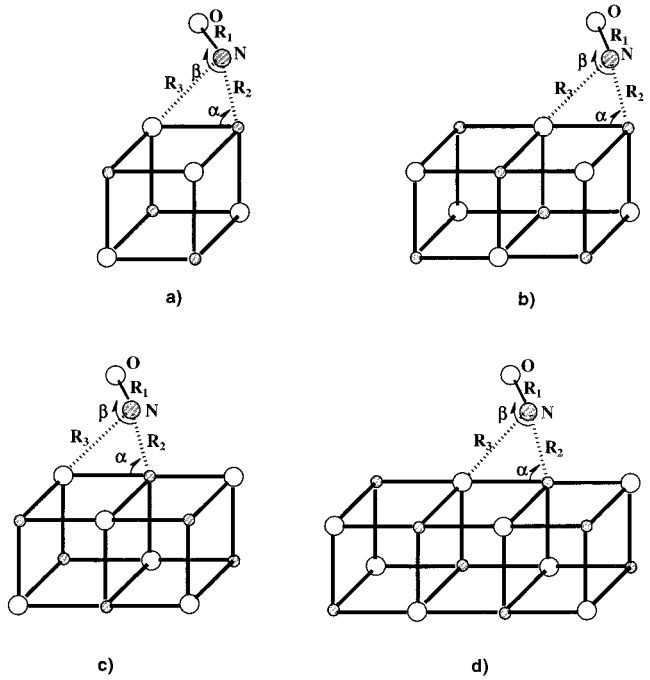

Figure 6. Bridge mode of monomeric NO adsorbed on the Mg_{XC}-O_{YC} (X,Y = 3,4) pair sites modeled by the embedded $(MgO)_n$ (n = 4, 6, 8) clusters. (The black dot is Mg, and the white circle is O.)

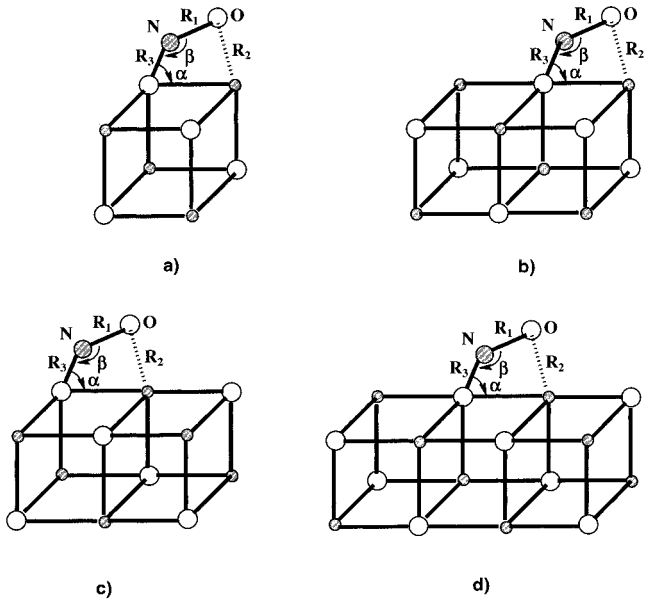

Figure 7. Chain mode of monomeric NO adsorbed on the Mg_{XC}-O_{YC} (X,Y = 3,4) pair sites modeled by the embedded $(MgO)_n$ (n = 4, 6, 8) clusters. (The black dot is Mg, and the white circle is O.)

between NO and the O_{YC} site. The distances between the O atoms of NO adspecies and Mg_{XC} sites are within 1.99−2.22 Å, close to the Mg_{XC}-O_{YC} lattice distance of 2.104 Å. The intramolecular N−O bond lengths (1.27−1.30 Å) are elongated by 0.11−0.14 Å with respect to free NO. All these suggest that NO adspecies in the chain mode are substantially activated.

In accordance with the above results, further Mulliken and NBO analyses reveal that, for NO adsorption in the chain mode over the low-coordinate Mg_{XC}-O_{YC} (X,Y = 3,4) pair sites, (a) a localized dative bond is formed between the empty 2π* of NO and the lone pair on the O_{XC} anion; (b) the intramolecular N−O bonding is considerably weakened with a net Mulliken charge on NO being around −0.60. Hence the adsorbed NO in the chain mode may be regarded as a NO^- adspecies; (c) the

TABLE 2: Optimized Geometries[a] for Monomeric NO Adsorptions on $(MgO)_n$ (n = 4, 6, 8) Embedded Clusters and Corresponding Adsorption Energies E_a (kcal/mol)[b]

n	pair site	mode	R_1 (Å)	R_2 (Å)	R_3 (Å)	α (°)	β (°)	Q_{NO}	E_a
4	Mg_{3C}-O_{3C}	bridge	1.177	2.102	2.109	60.2	173.1	−0.08	−17.9 (−17.7)
		chain	1.303	1.991	1.535	87.8	105.4	−0.57	−34.6 (−33.9)
6	Mg_{3C}-O_{4C}	bridge	1.173	2.130	2.259	64.5	169.4	+0.08	−10.6 (−10.5)
		chain	1.291	2.045	1.527	88.9	106.4	−0.54	−15.1 (−14.1)
	Mg_{4C}-O_{3C}	bridge	1.171	2.221	2.211	61.4	168.9	+0.01	−9.7 (−9.6)
		chain	1.267	2.086	1.625	89.1	103.8	−0.56	−12.0 (−11.5)
8	Mg_{4C}-O_{4C}	bridge	1.169	2.243	2.328	64.7	166.6	+0.02	−7.0 (−6.9)
		chain	1.266	2.222	1.562	94.0	105.2	−0.64	−5.5 (−4.6)

[a] For the nomenclature of the geometric parameters, please refer to Figures 6 and 7. [b] E_a = E(NO + cluster) − E(NO) − E(cluster). BSSE-corrected values are given in parentheses.

total charges on the (NO + O_{YC}) groups are around −1.75. Because the N−O_{YC} distances are as short as 1.53−1.63 Å, (NO + O_{YC}) could also be regarded as a bidentated NO_2^{2-} complex. Accordingly, the so-called NO^- and NO_2^{2-} surface species[8−13] suggested by the experimentalists might refer to the same surface species. Furthermore, the geometry of the NO_2^{2-} species implies that it may be an intermediate in the O-exchange reaction between NO and MgO solid, as suggested by Yanagisawa.[10]

Generally speaking, the more negative charge on NO adspecies there is, the longer N−O bond length is, and consequently the more strongly the intramolecular N−O bond is activated upon adsorption. As such, the capability of Mg_{XC}-O_{YC} (X,Y = 3,4) pair site to activate NO adsorbed in the chain mode (or in the bridge mode) could be assigned in the order Mg_{3C}-O_{3C} > Mg_{3C}-O_{4C} > Mg_{4C}-O_{3C} > Mg_{4C}-O_{4C}. This order coincides with that of the calculated binding energies. However, we should point out that there is no one-to-one correspondence between the strength of the adsorption bond and the activity of a (Mg_{XC}-O_{YC}) site. For example, NO adsorbed in the chain mode on Mg_{4C}-O_{4C}, though having the lowest binding energy (4.6 kcal/mol), is substantially activated, whereas NO adsorbed in the bridge mode on Mg_{3C}-O_{3C}, though having a large binding energy of 17.7 kcal/mol, is only weakly activated.

The IR frequencies of the NO adsorbed in the chain mode on O_{3C}-Mg_{3C} and O_{4C}-Mg_{3C} pair sites have been calculated by using bare cluster model of $(MgO)_4$ and $(MgO)_6$. Frequencies of 1227 cm^{-1} on O_{3C}-Mg_{3C} and 1287 cm^{-1} on O_{4C}-Mg_{3C} for the intramolecular N−O bond stretching were obtained. For NO adsorbed in the chain mode on other low-coordinated sites, N−O stretching frequencies slightly higher than 1227 cm^{-1} should be anticipated, because NO on those pair sites are less activated. This suggests that the experimentally detected absorption bands within 1250−1100 cm^{-1} [9] could, at least partially, be attributed to the intramolecular N−O bond stretching of NO adsorbed in the chain mode, that is, the NO_2^{2-} adspecies. Formation of NO_2^{2-} on CaO surface by adsorbing NO was shown theoretically, by Snis and Panas, to be plausible.[16] Their reg-CASSCF calculations predicted that on CaO, the intramolecular frequencies of NO adsorbed onto a terrace anion and onto a step-sitting anion are 1474 cm^{-1} and 1348 cm^{-1}, respectively.[16]

It is noteworthy that although the main low-coordinated pair sites available on MgO solid are the Mg_{4C}-O_{4C} pair sites, the binding between NO and Mg_{4C}-O_{4C} is too weak to ensure that NO adsorbed on such pair sites would be stable at RT. It seems that monomeric NO adsorption at the low-coordinate sites on MgO, either in the chain mode or in the bridge mode, could not account for the saturated NO coverage of 3−4% detected at RT.[9] Therefore, the surface complex NO_2^{2-} due to monomeric NO adsorption could not be the main, stable surface species on MgO at RT, though it could be an intermediate in the desorption process of the main, stable surface species. Indeed, Electron Spin Resonance (ESR) experiments[12,13] revealed that the amount of paramagnetic NO_2^{2-} surface species is just a percentage of the total loadings of NO on MgO at RT. On comparing the IR spectra of the NO/MgO system with those of the relevant inorganic salts, Platero et al. proposed the existence of $N_2O_2^{2-}$ and NO_2^- at the low-coordinate sites on MgO, which are products of a disproportionation reaction involving a low-coordinated surface anion.[9]

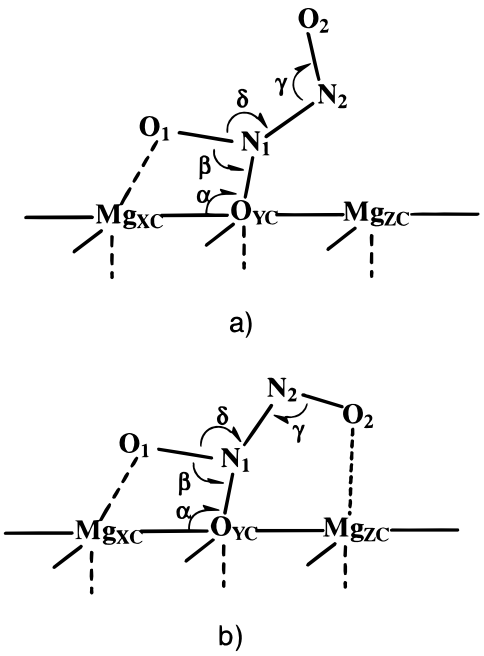

Figure 8. Two configurations of $N_2O_3^{2-}$ surface species, a) *cis*-$N_2O_3^{2-}$ and b) *trans*-$N_2O_3^{2-}$, on the low-coordinate Mg_{XC}-O_{YC} (X,Y = 3,4) pair sites modeled by embedded $(MgO)_n$ (n = 4,6,8) clusters. [All the so-formed $Mg_{XC}O_{YC}N_2O_2$ complexes are planar with a dihedral angle 135° between the molecular plane and the MgO(100)].

We suppose that the main, stable adspecies is in the form of $N_2O_3^{2-}$, which is formed by simply attaching another NO molecule onto the NO_2^{2-} intermediate. Actually, both NO_2^{2-} and free NO molecule have one spin-unpaired electron. It is likely for the two radical-like groups to couple with each other to form $N_2O_3^{2-}$ surface species. Similar $N_2O_3^{2-}$ surface species was postulated by Snis and Panas on CaO.[16] It is expected that the so-formed $N_2O_3^{2-}$ complexes have to be planar to facilitate the N−N π bonding along with the N−N σ bonding. Nonplanar form with only the N−N σ bonding should be energetically less favorable.

3.6. Surface Species $N_2O_3^{2-}$ Formed on Mg_{XC}-O_{YC} (X,Y = 3,4). Two planar forms of $N_2O_3^{2-}$ surface species have been located in our calculations, as depicted in Figure 8. For both configurations, the optimized dihedral angle between the mo-

TABLE 3: Optimized Geometries[a] of $N_2O_3^{2-}$ Surface Complexes and Corresponding Formation Energies (kcal/mol)[b]

site	mode	$O_{YC}N_1$ (Å)	N_1O_1 (Å)	N_1N_2 (Å)	N_2O_2 (Å)	α (°)	β (°)	δ (°)	γ (°)	E_1	E_2
$Mg_{3C}-O_{3C}$	cis	1.403	1.343	1.309	1.247	87.2	111.5	131.6	115.6	−12.3	−46.9
	trans	1.403	1.339	1.290	1.264	87.9	111.3	126.9	114.9	−15.8	−50.4
$Mg_{3C}-O_{4C}$	cis	1.405	1.308	1.311	1.244	86.9	114.4	111.9	119.6	−15.3	−30.4
	trans	1.511	1.303	1.266	1.292	81.7	113.4	124.6	118.2	−23.6	−38.7
$Mg_{4C}-O_{3C}$	cis	1.406	1.322	1.307	1.252	89.8	110.5	133.7	115.5	−8.9	−20.9
	trans	1.404	1.319	1.287	1.272	91.0	110.4	129.1	114.9	−14.5	−26.5
$Mg_{4C}-O_{4C}$	cis	1.419	1.288	1.311	1.249	88.4	114.2	134.4	119.2	−16.0	−21.5
	trans	1.554	1.279	1.263	1.296	82.8	111.9	124.1	119.2	−22.7	−28.2

[a] For the nomenclature of the geometric parameters, please refer to Figure 8. [b] $E_1 = E[(NO)_2 + \text{cluster}] - E(NO) - E[NO + \text{cluster}]$; $E_2 = E[(NO)_2 + \text{cluster}] - 2E(NO) - E(\text{cluster})$.

TABLE 4: Calculated IR Frequencies of $N_2O_3^{2-}$ Surface Complexes as Well as Experimental IR Spectra of NO/MgO Chemisorption System, $N_2O_3^{2-}$ in Solid $Na_2N_2O_3$, $N_2O_2^{2-}$ in Solid $Na_2N_2O_2$, and NO_2^- in $NaNO_2$

		NO/MgO chemisorption system				$N_2O_3^{2-}$ in $Na_2N_2O_3$	$N_2O_2^{2-}$ in $Na_2N_2O_2$	NO_2^- in $NaNO_2$
		present work		exptl				
		a	*b*	77 K	RT	expt.[25]	expt.[25]	expt.[25]
ν_1	antisym. NO_2 stretch	1472	1534	1450−1350	1500−1350	1400		ν_1 1337
ν_2	sym. NO_2 stretch	1415	1269	1313	1250−1100	1280	ν_1 1313	
ν_3	N−N stretch	1097	1110	1250−1100		1120		ν_2 1270
ν_4	NO stretch	917		893		975	ν_2 1047	ν_3 829

[a] ν_1: N−N stretch; ν_2: N−O sym. stretch. [b] ν_1: N−O bonds sym. stretch; ν_2: N−O bonds antisym. stretch; ν_3: ONO bend.

lecular plane of $N_2O_3^{2-}$ group and the MgO(100) surface is 135°. As these complexes can also be regarded as an N_2O_2 molecule adsorbed on an O_{YC}2- (Y = 3,4) anion, we refer to the two configurations of $N_2O_3^{2-}$ surface complexes as *cis*- and *trans*-$N_2O_3^{2-}$, with respect to *cis*-N_2O_2 and *trans*-N_2O_2, respectively. The geometrical parameters of the $N_2O_3^{2-}$ surface species and the corresponding binding energies are given in Table 3.

The process of attaching an NO molecule onto the NO_2^{2-} species is calculated to be exothermic, with the energy gain ranging from 9 kcal/mol to 24 kcal/mol, depending on the configuration formed and the type of pair sites. The N−N bond lengths in these $N_2O_3^{2-}$ complexes are within the range of 1.26−1.32 Å, which clearly indicates that the bond between the NO_2^{2-} adspecies and the second NO is rather covalent. On a given Mg_{XC}-O_{YC} pair site, the trans form is more stable than the cis form, and the N−N double bonding is stronger in the trans form than that in the cis form, as implied by the shorter N−N bond length in the trans form. In particular, on the Mg_{4C}-O_{4C} pair site, the formation energy of NO_2^{2-} species is only −5.5 kcal/mol, whereas the formation energies of *cis*-$N_2O_3^{2-}$ and *trans*-$N_2O_3^{2-}$ species are −21.5 kcal/mol and −28.8 kcal/mol, respectively, with respect to two free NO molecules. That is, the NO_2^{2-} intermediate could be substantially stabilized as long as the second NO molecule is attached onto it. It seems that at low temperature (77 K) with high NO coverage, both *cis*- and *trans*-$N_2O_3^{2-}$ surface species may exist, whereas at RT with low coverage, *trans*-$N_2O_3^{2-}$ surface species should be preferred.

Furthermore, the distance between the O_1 atom in the *cis*-$N_2O_3^{2-}$ surface species and the nearest step-sitting Mg cation is around 2.1 Å, whereas in *trans*-$N_2O_3^{2-}$, both the O_1 and O_2 atoms are close to the step-sitting Mg^{2+} cations, with the Mg−O1(2) distances around 1.95 Å. Accordingly, we reckon, on the basis of the structures of these $N_2O_3^{2-}$ surface complexes, that at elevated temperature the $N_2O_3^{2-}$ surface complex would possibly decompose to N_2O, and especially in the trans form it may also decompose to N_2 provided that the temperature is high enough. The product N_2O may further decompose to N_2 and O_2 on the low-coordinate Mg_{XC}-O_{YC} (X,Y = 3,4) pair sites, as demonstrated by our previous theoretical study regarding N_2O decomposition on MgO solid.[38] We will present the energetics of this mechanism in a later section.

3.7. IR Frequencies of $N_2O_3^{2-}$ Surface Species. We have calculated the IR frequencies of the *cis*- and *trans*-$N_2O_3^{2-}$ surface species formed on the Mg_{4C}-O_{4C} pair site with bare cluster model of $(MgO)_8$. The calculated frequencies in the range of 1550−800 cm^{-1} are listed in Table 4.

For comparison, the experimental IR frequencies in the same range reported by Platero et al.[9] are also included in Table 4. On comparing the IR spectra of NO/MgO chemisorption system with those of *cis*-$N_2O_2^{2-}$ (e.g., in solid $Na_2N_2O_2$) and NO_2^- (e.g., in solid $NaNO_2$), Platero et al. interpreted the IR spectra of the NO/MgO chemisorption system as follows: (a) the two broad bands in the range of 1450−1350 cm^{-1} and 1250−1100 cm^{-1} were ascribed to NO_2^- surface species, whereas the absorption bands at 1313 cm^{-1} and 893 cm^{-1} detectable only at low temperature (77 K) were attributed to *cis*-$N_2O_2^{2-}$; (b) the feature that the latter absorption bands decrease upon outgassing at 77 K and disappear upon heating to RT is due to decomposition of *cis*-$N_2O_2^{2-}$ surface species.

In Table 4, the experimental IR frequencies of some relevant nitrogen oxides[36] are also given. These are for $N_2O_3^{2-}$ in solid $Na_2N_2O_3$, *cis*-$N_2O_2^{2-}$ in solid $Na_2N_2O_2$, and NO_2^- in solid $NaNO_2$. It seems to us that it is more reasonable to compare the IR spectra of the NO/MgO system with the IR spectra of $N_2O_3^{2-}$ ($Na_2N_2O_3$) species, than with those of NO_2^- and *cis*-$N_2O_2^{2-}$ anions. It is thus not surprising that our calculated IR frequencies of the *cis*- and *trans*-$N_2O_3^{2-}$ surface species are in good agreement with the IR spectra of NO/MgO system in the range of 1500−800 cm^{-1}. Furthermore, our calculations demonstrate that the specific feature[9] that the absorption bands at 1313 cm^{-1} and 893 cm^{-1} detectable at 77 K disappear at RT would be attributed to the configuration transformation from *cis*-$N_2O_3^{2-}$ to *trans*-$N_2O_3^{2-}$.

Formation of the *cis*-$N_2O_3^{2-}$ surface species on CaO was also revealed by Snis and Panas recently.[16] The frequencies of the *cis*-$N_2O_3^{2-}$ were calculated, by means of the reg-CASSCF method, to be 1543, 1441, 1243, and 978 cm^{-1} for the species formed at a five-coordinate anion site and to be 1482, 1413, 1377, and 897 cm^{-1} for the species formed at a step-sitting anion site. For comparison, only the values higher than 800 cm^{-1} are cited here. These values are comparable with our calculated

values, except that the frequency of the N−N bond stretch is much higher than our B3LYP values.

3.8. Mechanism of NO Decomposition Reaction on Metal Oxides. A possible mechanism of NO decomposition on MgO via the $N_2O_3^{2-}$ surface species is given as follows:

$$\text{total reaction: } 2NO \rightarrow N_2O + 1/2\ O_2\ (g)\ \Delta E = -25.8\ \text{kcal/mol}$$

$$NO(g) + [O_{XC}]^{2-}\ (s) \rightarrow [NO_2]^{2-}\ (ads)\ \Delta E_1 = -5.5\ \text{kcal/mol} \quad (1)$$

$$NO(g) + [NO_2]^{2-}\ (ads) \rightarrow [N_2O_3]^{2-}(ads)\ \Delta E_2 = -22.7\ \text{kcal/mol} \quad (2)$$

$$[N_2O_3]^{2-}(ads) \rightarrow N_2O\ (g) + [O_2]^{2-}\ (ads)\ \Delta E_3 = 13.0\ \text{kcal/mol} \quad (3)$$

$$[O_2]^{2-}\ (ads) \rightarrow 1/2\ O_2\ (g) + [O_{XC}]^{2-}(s)\ \Delta E_4 = -10.6\ \text{kcal/mol} \quad (4)$$

Here the reaction heat of each step was calculated by assuming the process occurs on the step-sitting Mg_{4C}-O_{4C} pair site and via the *trans*-$N_2O_3^{2-}$ intermediate. The binding energy of atomic oxygen on the Mg_{4C}-O_{4C} pair site was calculated to be 49.8 kcal/mol in our previous work.[38] In this proposed reaction route, only step 3 is endothermic, with a reaction heat of 13.0 kcal/mol. This could be correlated with the experimentally determined activation energy of 11.2 kcal/mol for N_2O desorption from the NO/MgO chemisorption system.[10]

According to this reaction route, decomposition of $N_2O_3^{2-}$ to N_2O would leave oxygen adspecies on the active sites. Further decomposition of the N_2O to N_2 would also leave oxygen species on the active sites. Temperature Programmed Desorption (TPD) experiments of Nakamura et al. revealed that the desorption of oxygen adspecies requires an activation energy of ∼34 kcal/mol,[39] implying that the existence of O_2 in the reaction may retard the reaction of NO decomposition on MgO. Indeed, Winter did find experimentally the retardation effect of O_2 to the reaction of NO decomposition on a variety of metal oxides.[6]

We should mention another possible reaction route in which superficial anionic vacancies or F-centers were proposed to be the active sites for NO decomposition on metal oxides.[5,7,16] Electrons localized in the superficial anionic vacancies or F-centers would work to form anionic N_2O_2 with the incoming NO molecules. The so-formed anionic N_2O_2 then decomposes to form N_2O. For clarity, we refer to this reaction route as vacancy-based route, and the reaction route we proposed in the preceding paragraph as vacancy-free route. When we were preparing this manuscript, Snis and Panas reported their quantum chemical study regarding anionic NO and N_2O_2 adspecies on prereduced CaO surface, in which the vacancy-based route was supposed to be plausible.[16] Since decomposition of anionic N_2O_2 formed in the vacancy-based route will leave O^{2-} to occupy the anionic vacancy, a reduction treatment of the metal oxides to reproduce anionic vacancies is thus mandatory to keep the reaction proceeding cyclically. In fact, experiments regarding extraction of superficial oxygen by using reductive CO and H_2 gases and the effect of CO and H_2 to NO decomposition on CaO were reported by Acke et al.[7]

The role of reductive gases such as CO and H_2 for both the vacancy-based route and the vacancy-free route is obvious. In the vacancy-free route, reductive gases help to reduce the activation energy of the desorption of oxygen adspecies, whereas in the vacancy-based route, they work to extract lattice oxygen to reproduce the active vacancies. An advantage of the vacancy-free route is that it could proceed cyclically upon heating without the help of reductive gases as shown by the experiments.[5,6,8−11] Both routes should work competitively when there exist the reductive gases in the reaction system.

3.9. NO Adsorption on MgO and CaO: Similarities and Differences. The present work disclosed the formation of NO_2^{2-} and $N_2O_3^{2-}$ surface species on the low-coordinate anions upon NO adsorption. We noted that similar surface species were found on CaO solid by Snis and Panas in their ab initio study.[16] Some similarities and differences between MgO and CaO in their reactivity toward NO are addressed as follows.

On both metal oxides, NO can be adsorbed at the low-coordinate O^{2-} sites, giving rise to NO_2^{2-} species. The bonding between NO and the low-coordinate O^{2-} is covalent and involves charge transfer from the lone pair on the O_{XC} anion to the empty $2\pi^*$ MO of NO. The lower coordination number the surface anion has, the more easily the charge transfer occurs and the higher reactivity the anion shows toward the incoming NO. The reason for this trend is that the Madelung potential at an anionic site with lower coordination number is smaller, and hence the anion with lower coordination number is less stabilized.[40] Consequently, the electron cloud of the anion with lower coordination number is more spatially diffuse, and can overlap more efficiently with the $2\pi^*$ MO of the incoming NO.

CaO shows higher reactivity toward NO than does MgO. This remark is evidenced by our theoretical finding that on MgO(001) surface the interaction between NO and a five-coordinate anion is virtually repulsive and the theoretical finding of Snis and Panas[16] that on CaO(001) the adsorption of NO over a five-coordinate anion to form an NO_2^{2-} anion is energetically favorable (with the calculated binding energy of ∼6 kcal/mol). Further evidence is that the formation energy of NO_2^{2-} at an edge site on CaO (−12 /−19 kcal/mol by Snis and Panas[16]) is larger than that of NO_2^{2-} formed over the similar site on MgO (−4.6 kcal/mol in present work). The lattice distance in CaO is longer than that in MgO so that the Madelung potential at an anion site on CaO is smaller than that on MgO.[40]

Formation of $N_2O_3^{2-}$ seems unfeasible at a five-coordinate terrace anion site on MgO(001), but feasible at a terrace anion site of CaO(001). At low-coordinate anion sites of both metal oxides, stable $N_2O_3^{2-}$ surface species are formed. Here we report two isomers of $N_2O_3^{2-}$ surface species, whereas Snis and Parker considered only the *cis*-$N_2O_3^{3-}$ surface species. We believe that at low-coordination anion sites on CaO, the formation of *trans*-$N_2O_3^{2-}$ surface species should also be easier than that of *cis*-$N_2O_3^{2-}$ surface species.

4. Concluding Remarks

In the present paper, a quantum chemical study based on hybrid density functional theory and embedded cluster model method has been performed to explore the chemistry of NO on MgO solid. Both monomeric and dimeric adsorptions of NO on terrace, step, and corner sites have been considered. On terrace sites, only weakly physisorbed NO and *cis*-N_2O_2 adspecies were found, whereas at low-coordinated Mg_{XC}-O_{YC} (X,Y = 3,4) pair sites on steps and corners, two adsorption modes, namely bridge mode and chain mode, were found for monomeric NO adsorption. NO adsorbed in the chain mode is highly activated, leading to the formation of NO_2^{2-} surface species. The NO_2^{2-} surface species could be involved as an intermediate in O-exchange reaction between NO and MgO solid

and in the desorption process. We proposed, for the first time, and verified theoretically the existence of the stable surface species $N_2O_3^{2-}$ in the NO/MgO adsorption system. The $N_2O_3^{2-}$ surfaces species could be a pivot intermediate in the reaction of NO decomposition on MgO solid. The calculated IR frequencies of the $N_2O_3^{2-}$ surface species and the *cis*-N_2O_2 adspecies are in agreement with the experimental IR spectra of NO/MgO chemisorption system, and account well for the specific temperature dependence of IR spectra.

On the basis of the structures of the $N_2O_3^{2-}$ surface species, a new mechanism of the NO decomposition reaction has been proposed. At elevated temperature, $N_2O_3^{2-}$ could decompose to form N_2O or N_2 and O_2. The advantages and disadvantages of this mechanism have been discussed, after comparing this vacancy-free mechanism with the vacancy-based mechanism.

Acknowledgment. This work is supported by the National Nature Science Foundation of China, the doctoral project foundation of the State Education Commission of China, and *Fok Ying Dung* research foundation. X.L. thanks Dr. Snis at Göteborg University for providing his in-press paper.

References and Notes

(1) Wendelken, J. F. *Appl. Surf. Sci.* **1982**, *11/12*, 172.
(2) Johnson, D. W.; Matloob, M. H.; Roberts, M. W. *J. Chem. Soc., Chem. Commun*. **1978**, 40.
(3) Masel, R. I.; Umbach, E.; Fuggle, J. C.; Menzel, D. *Surf. Sci.* **1979**, *79*, 26.
(4) Brown, W. A.; Gardner, P.; King D. A. *J. Phys. Chem*. **1995**, *99*, 7065.
(5) Winter, E. R. S. *J. Catal.* **1971**, *22*, 158.
(6) Winter, E. R. S. *J. Catal.* **1974**, *34*, 440.
(7) Acke, F.; Panas, I.; Strömberg, D. *J. Phys. Chem. B* **1997**, *101*, 6484.
(8) Cerruti, L.; Modone, E.; Guglielminotti, E.; Borello, E. *J. Chem. Soc., Faraday Trans. 1* **1974**, *70*, 729.
(9) Platero, E. E.; Spoto G.; Zecchina A. *J. Chem. Soc., Faraday Trans. 1* **1985**, *81*, 1283.
(10) Yanagisawa, Y. *Appl. Surf. Sci.* **1995**, *89*, 251.
(11) Luo, M.; Zhou, L.; Ding, Y.; Yuan, X.; Zhang, X. *Indian J. Chem. A* **1996**, *37*, 53.
(12) Lunsford, J. K. *J. Chem. Phys.* **1967**, *46*, 4347.
(13) Zhang, G.; Tanaka, T.; Yamaguchi, T.; Hattori, H.; Tanabe, K. *J. Phys. Chem.* **1990**, *94*, 506.
(14) Garrone, E.; Giamello, E. In *Studies in Surface Science and Catalysis 21: Adsorption and Catalysis on Oxide Surfaces*; Che, M.; Bond, G. C., Eds.; Elsevier Sicence Publishers: Amsterdam, 1985; p 225.
(15) Lu, X.; Xu, X.; Wang, N.; Zhang, Q. *Chem. Res. Chin. Univ.* **1998**, *14*, 215.
(16) Snis, A.; Panas, I. *Surf. Sci.* **1998**, *412*−*413*, 477.
(17) Wyckoff, R. W. G. *Crystal Structures*; Wiley: New York, 1963.
(18) Stevens, W. J.; Basch, H.; Krauss, M. *J. Chem. Phys.* **1984**, *81*, 6026.
(19) Xu, X.; Nakatsuji, H.; Ehara, M.; Lu, X.; Wang, N.; Zhang, Q. *Sci. China Ser. B* (in English) **1998**, *41*, 113.
(20) Becke, A. D. *J. Chem. Phys.* **1993**, *98*, 5648.
(21) Lee, C.; Yang, W.; Parr, R. G. *Phys. Rev.* **1988**, *B37*, 785.
(22) Frisch, M. J.; Trucks, G. W.; Schlegel, H. B.; Gill, P. M. W.; Johnson, B. G.; Robb, M. A.; Cheeseman, J. R.; Keith, T.; Petersson, G. A.; Montgomery, J. A.; Raghavachari, K.; Al-Laham, M. A.; Zakrzewski, V. G.; Ortiz, J. V.; Foresman, J. B.; Peng, C. Y.; Ayala, P. Y.; Chen, W.; Wong, M. W.; Andres, J. L.; Replogle, E. S.; Gomperts, R.; Martin, R. L.; Fox, D. J.; Binkley, J. S.; Defrees, D. J.; Baker, J.; Stewart, J. P.; Head-Gordon, M.; Gonzalez, C.; Pople, J. A. *Gaussian 94*; Gaussian, Inc.: Pittsburgh, PA, 1995.
(23) Herzberg, G. *Electronic Spectra of Polyatomic Molecules*; Van Nostrand Reinhold: New York, 1966.
(24) Boys, S. F.; Bernard, F. *Mol. Phys.* **1970**, *19*, 553.
(25) Pelmenschikov, A. G.; Morosi, G.; Gamba, A.; Coluccia, S. *J. Phys. Chem.* **1995**, *99*, 15018.
(26) Benzel, M. A.; Dykstra, C. E.; Vincent, M. A. *Chem. Phys. Lett.* **1981**, *78*, 139.
(27) Ha, T. K. *Theor. Chim. Acta* **1981**, *58*, 125.
(28) Lee, T. J.; Rice, J. E.; Scuseria, G. E.; Schaefer, H. F. III. *Theor. Chim. Acta* **1989**, *75*, 81.
(29) Stirling, A.; Papai, I.; Mink, J.; Salahub, D. R. *J. Chem. Phys.* **1994**, *100*, 2910.
(30) Jursic, B. S. *Chem. Phys. Lett.* **1995**, *236*, 206.
(31) Jursic, B. S.; Zdravkovski, Z. *Int. J. Quantum Chem.* **1995**, *54*, 161.
(32) Canty, J. F.; Stone, E. G.; Bach, S. B. H.; Ball, D. W. *Chem. Phys.* **1997**, *216*, 81.
(33) Snis, A.; Panas, I. *Chem. Phys.* **1997**, *221*, 1.
(34) Duarte, H. A.; Salahub, D. R. *J. Phys. Chem. B* **1997**, *101*, 7464.
(35) Duarte, H. A.; Proynov, E.; Salahub, D. R. *J. Chem. Phys.* **1998**, *109*, 26.
(36) Laane, J.; Ohlsen, J. R. *Prog. Inorg. Chem.* **1980**, *27*, 465 and references therein.
(37) Carpenter, J. E.; Weinhold, F. *J. Mol. Struct. (THEOCHEM)* **1988**, *169*, 41.
(38) Lu, X.; Xu, X.; Wang, N.; Zhang, Q. *J. Phys. Chem. B*, submitted.
(39) Nakamura, M.; Yanagibishi, H.; Mitsuhashi, H.; Takezawa, N. *Bull. Chem. Soc. Jpn.* **1993**, *66*, 2467.
(40) Pacchioni, G.; Ricart, J. M.; Illas, F. *J. Am. Chem. Soc.* **1994**, 116, 10152.